



Central role of electronic temperature for photoelectron charge and spin mobilities in p + -GaAs

Fabian Cadiz, D. Paget, A. Rowe, Emilien Peytavit, S. Arscott

► To cite this version:

Fabian Cadiz, D. Paget, A. Rowe, Emilien Peytavit, S. Arscott. Central role of electronic temperature for photoelectron charge and spin mobilities in p + -GaAs. Applied Physics Letters, 2015, 106 (9), pp.092108. 10.1063/1.4914357 . hal-02345533

HAL Id: hal-02345533

<https://hal.science/hal-02345533>

Submitted on 27 May 2022

HAL is a multi-disciplinary open access archive for the deposit and dissemination of scientific research documents, whether they are published or not. The documents may come from teaching and research institutions in France or abroad, or from public or private research centers.

L'archive ouverte pluridisciplinaire **HAL**, est destinée au dépôt et à la diffusion de documents scientifiques de niveau recherche, publiés ou non, émanant des établissements d'enseignement et de recherche français ou étrangers, des laboratoires publics ou privés.

Central role of electronic temperature for photoelectron charge and spin mobilities in p^+ -GaAs

Cite as: Appl. Phys. Lett. **106**, 092108 (2015); <https://doi.org/10.1063/1.4914357>

Submitted: 28 January 2015 • Accepted: 25 February 2015 • Published Online: 06 March 2015

F. Cadiz, D. Paget, A. C. H. Rowe, et al.



View Online



Export Citation



CrossMark

ARTICLES YOU MAY BE INTERESTED IN

[Absence of carrier separation in ambipolar charge and spin drift in \$p^+\$ -GaAs](#)

Applied Physics Letters **107**, 162101 (2015); <https://doi.org/10.1063/1.4933189>

[All optical method for investigation of spin and charge transport in semiconductors: Combination of spatially and time-resolved luminescence](#)

Journal of Applied Physics **116**, 023711 (2014); <https://doi.org/10.1063/1.4889799>

[Spin and recombination dynamics of excitons and free electrons in p-type GaAs: Effect of carrier density](#)

Applied Physics Letters **110**, 082101 (2017); <https://doi.org/10.1063/1.4977003>

Lock-in Amplifiers up to 600 MHz



Zurich
Instruments



Central role of electronic temperature for photoelectron charge and spin mobilities in p^+ -GaAs

F. Cadiz,^{1,a)} D. Paget,¹ A. C. H. Rowe,¹ E. Peytavit,² and S. Arscott²

¹Physique de la Matière Condensée, Ecole Polytechnique, CNRS, 91128 Palaiseau, France

²Institut d'Electronique, de Microélectronique et de Nanotechnologie (IEMN), University of Lille, CNRS, Avenue Poincaré, Cité Scientifique, 59652 Villeneuve d'Ascq, France

(Received 28 January 2015; accepted 25 February 2015; published online 6 March 2015)

The charge and spin mobilities of minority photoelectrons in p^+ -GaAs are determined by monitoring the effect of an electric field on the spatial profiles of the luminescence and of its polarization. By using electric fields to increase the photoelectron temperature T_e without significantly changing the hole or lattice temperatures, the charge and spin mobilities are shown to be principally dependent on T_e . For $T_e > 70$ K, both the charge and spin mobilities vary as $T_e^{-1.3}$, while at lower temperatures this changes to an even more rapid $T_e^{-4.3}$ law. This finding suggests that current theoretical models based on degeneracy of majority carriers cannot fully explain the observed temperature dependence of minority carrier mobility. © 2015 AIP Publishing LLC. [<http://dx.doi.org/10.1063/1.4914357>]

Understanding the mechanisms which limit the minority carrier charge mobility μ_e and spin mobility μ_s in semiconductors is necessary for the correct design of bipolar charge and spin devices. The electron mobility in p-type GaAs features a completely different temperature dependence than that of majority electrons in n-GaAs for a similar doping level.^{1–3} A number of possible reasons for this have been discussed in the literature, including carrier freezeout at high hole concentrations,^{4,5} screening of ionized impurities,⁶ and increasing hole degeneracy as temperature is lowered.⁷

Here, we experimentally measure the minority electron mobility as a function of lattice temperature T_L and electronic temperature T_e of p^+ -GaAs. The ability to change T_e without changing T_L using an applied electric field is used to demonstrate that the charge and spin mobilities are primarily determined by T_e . The sample consists of a $3\ \mu\text{m}$ thick, carbon doped material ($N_A = 10^{18}\text{cm}^{-3}$). A 100 nm thick GaInP epilayer between the semi-insulating substrate and the active layer ensures that recombination at the interface is negligible. As shown in Fig. 1(a), a Hall bar was photolithographically etched into the active layer. Fig. 1(b) shows the dependence as a function of the lattice temperature (T_L) of the resistivity, the majority hole concentration, and the mobility. The density of ionized acceptors is only weakly temperature dependent for this doping level since the impurity band and the valence band are merged into a continuum of states.^{4,5} The hole mobility at room temperature, $\mu_h = 202\text{cm}^2\text{V}^{-1}\text{s}^{-1}$, as well as its $\sim T_L^{1/2}$ temperature dependence below 100 K are in good agreement with previous reports on similarly doped GaAs.^{5,9,10}

Spin-polarized photoelectrons were generated by a tightly focussed circularly polarized CW laser excitation (1/e half width of $0.6\ \mu\text{m}$, energy 1.59 eV unless otherwise stated) in a setup described elsewhere.¹¹ A maximum excitation power of 0.01 mW produces a non degenerate photoelectron concentration of $\sim 5 \times 10^{14}\text{cm}^{-3}$ in the steady state. The

temperature T_e was monitored from the high energy tail of the luminescence spectrum. This spectrum was obtained using a multimode optical fiber placed in the image plane

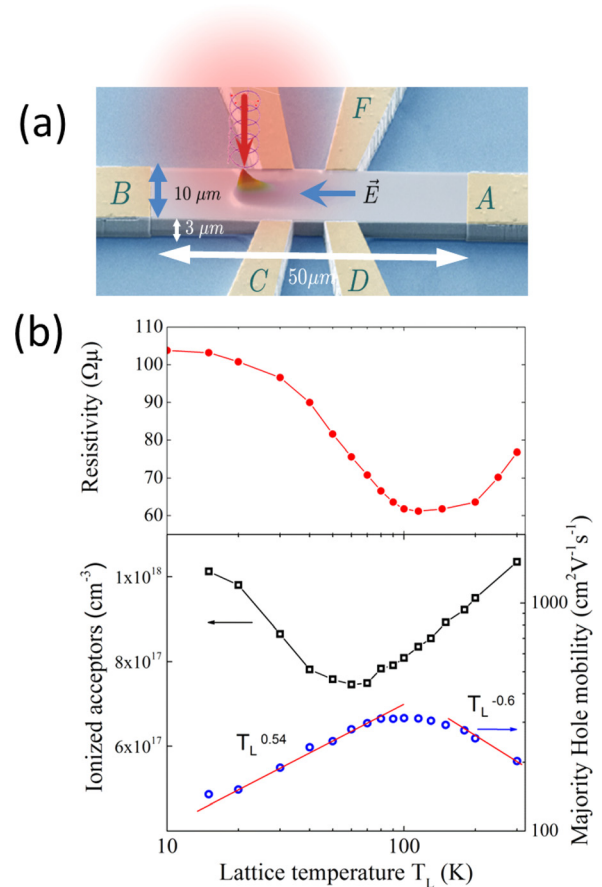


FIG. 1. (a) SEM image of the p-GaAs hall bar used to study both minority and majority carrier transport. Also shown is a 3D representation of a measured electron density profile when an electric field is applied. (b) Dependence as a function of lattice temperature of the resistivity (plain circles), the concentration of ionized acceptors (open squares), and their mobility (open circles).

^{a)}fabian.cadiz@polytechnique.edu

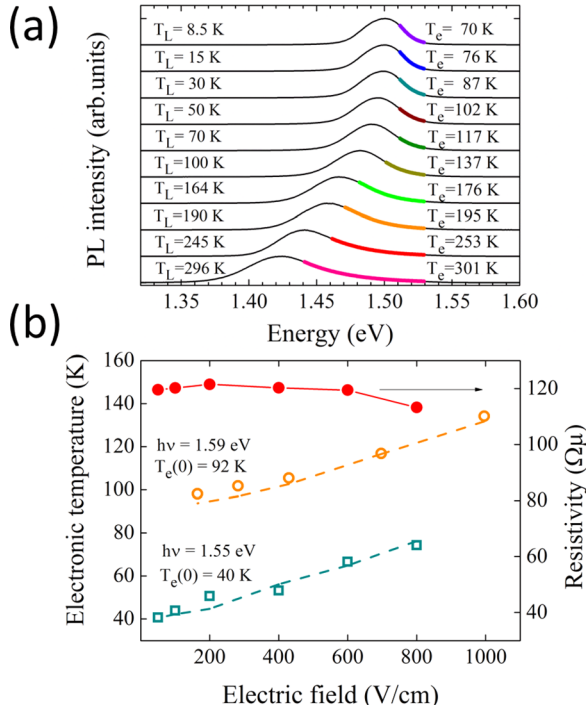


FIG. 2. (a) Normalized luminescence spectra for different lattice temperatures. Fits of the high energy tail of the spectra (shown by thicker lines) are used to estimate the electronic temperature T_e . (b) Measured T_e as a function of applied electric field for laser excitation energies of 1.55 eV and 1.59 eV, respectively. The increase of T_e as a function of E is well explained by Eq. (1) which assumes an energy-independent energy-relaxation time of 1.5 ps (dotted line) and 1.2 ps (solid line) for each case. Also shown in the bottom panel (plain circles) is the electric field dependence of the resistivity, which shows that the hole temperature is not affected by the electric field.

and its shape does not depend on space. As shown in Fig. 2(a), taken at a low electric field of $E = 200$ V/cm, T_e significantly differs from T_L when the latter is below 100 K.

In this work, application of electric fields small enough to avoid intervalley transitions^{12,13} allows us to increase T_e without changing the hole temperature. This is shown in Fig. 2(b) which gives the electric field dependences of $T_e(E)$ for two laser excitation energies, of 1.55 eV and 1.59 eV. In these two cases, the temperatures at zero field, related to the loss of energy to the phonons, are $T_e(0) = 40$ K and $T_e(0) = 92$ K, respectively. Combination of the two excitation energies gives access to $40 \text{ K} < T_e < 130$ K. The lines in Fig. 2(b) are predictions based on the following simple balance equation for the power delivered to the electron gas by the electric field:

$$\frac{3}{2}k_B[T_e(E) - T_e(0)] = qv_dE\tau_E, \quad (1)$$

where k_B is Boltzmann's constant and q is the electronic charge. The quantity $v_d = \mu_e E$ is the drift velocity and τ_E is the energy relaxation time. The data are well explained by an energy-independent relaxation time of $\tau_E = 1.2$ ps and $\tau_E = 1.5$ ps for initial electron temperatures of $T_e(0) = 40$ K and $T_e(0) = 92$ K, respectively. These values are an order of magnitude larger than values measured at 300 K,¹² consistent with a significant decrease of the energy relaxation rate at lower temperatures due to less efficient phonon scattering. Note that, as also shown in Fig. 2(b), in the same conditions

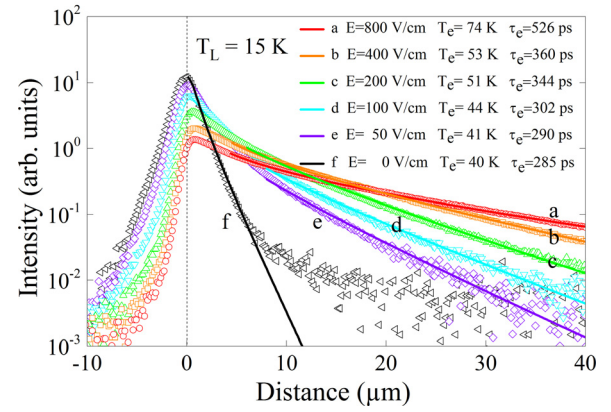


FIG. 3. Charge density profiles at $T_L = 15$ K for selected values of the electric field (and hence T_e). Dotted lines are fits obtained with Eq. (2) that give the $\mu_e\tau_e$ product for the charge distribution. The mobility is obtained using the values of τ_e measured independently and also shown in the figure.

the sample resistivity very weakly changes. Since for a local light excitation, this resistivity is dominated by the hole contribution, this result shows that the hole temperature (T_h) remains unchanged. This can be understood by using Eq. (1), and taking a hole mobility at least 10 times lower than the electron one and phonon emission times for holes twice as short.¹⁹ Moreover, since the photogenerated hole concentration is much smaller than N_A , it is concluded that $T_h \approx T_L$ in all the experiments reported here.

The minority carrier mobility μ_e is determined by imaging the spatial dependence of the luminescence, which is proportional to the electron concentration n .¹¹ Fig. 3 shows sections of these images along the direction of the electric field for $T_L = 15$ K. Drift of the electrons in the applied electric field leads to a significant change of the profiles which are well approximated by the 2-dimensional diffusion result²

$$n(x) \propto e^{(\mu_e\tau_e E x)/(2D_e\tau_e)} K_0 \left[\frac{\sqrt{(\mu_e\tau_e E)^2 + 4D_e\tau_e}}{2D_e\tau_e} x \right], \quad (2)$$

where D_e and τ_e are the electron diffusion constant and lifetime, respectively, and K_0 is a modified Bessel function of the second kind. In a nondegenerate electron gas, the Einstein relation, $D_e = [k_B T_e / q] \mu_e$, is valid so that the only fitting parameter in Eq. (2) is the $\mu_e\tau_e$ product. An independent time-resolved photoluminescence characterization of the sample was made in order to measure τ_e as a function of electron temperature¹⁴ and the values of τ_e corresponding to the various curves of Fig. 3 are also shown in this figure. Thus, a fit of the luminescence intensity profile with Eq. (2) yields an estimate for μ_e . At $T_L = 300$ K, $\mu_e = 1560 \text{ cm}^2 \text{V}^{-1} \text{s}^{-1}$, in excellent agreement with the theoretical value of $1643 \text{ cm}^2 \text{V}^{-1} \text{s}^{-1}$ at similar doping densities predicted by Bennett¹⁵ and with the existing experimental data.^{19,10,16} The spin mobility μ_s was measured using a similar approach by using a circularly polarized excitation and a quarter wave plate followed by a linear polarizer at the reception, thus yielding the profile of the spin concentration $s = n_+ - n_-$, where n_{\pm} is the concentration of electrons of spin \pm , with a quantization axis along the direction of light excitation.¹¹ The equation for s is similar to Eq. (2) where D_e and τ_e are replaced by their spin counterparts

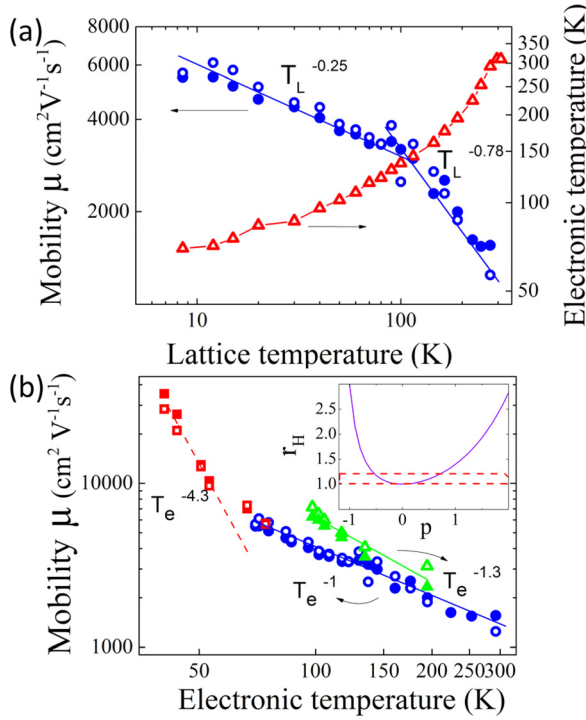


FIG. 4. (a) The measured electron (solid circles) and spin (open circles) mobilities, μ_e and μ_s , for an electric field of 200 V/cm as a function of T_L . In this case, as shown by the variation of T_e , shown by open triangles, both T_e and T_L vary. (b) Same data as panel a plotted against T_e (solid circles and open circles for μ_e and μ_s , respectively). This curve shows a $1/T_e$ variation at high temperature. Also shown are the dependences of μ_e and μ_s , at fixed T_L , found by varying T_e using the electric field only. The solid triangles correspond to μ_e for $T_L \approx 30-40$ K and an electric field varying between 200 and 1300 V/cm. The solid and open squares correspond to μ_e and μ_s at a lower T_e ($T_L = 15$ K). A dramatic increase of the mobility is observed, with a $1/T_e^{4.3}$ dependence. The inset of the bottom panel shows the expected dependence of r_H (Eq. (4)) on the exponent p in Eq. (3).

D_s and τ_s . Using the predetermined value of the spin lifetime, τ_s (Ref. 14), an estimation of μ_s is possible.

The results are summarized in Fig. 4. The charge (full circles) and spin (open circles) mobilities as a function of T_L for a fixed electric field of 200 V/cm are first shown in Fig. 4(a). It is found that μ_e and μ_s are equal within experimental error at all temperatures, thus verifying predictions for a non-degenerate electron gas in the absence of spin-dependent momentum relaxation mechanisms.¹⁷ For $T_L > 100$ K, μ_e varies as $T_L^{-0.78}$ close to the $1/T_L$ behaviour previously reported in this temperature range.¹ This exponent is reduced to -0.25 for $T_L < 100$ K. Fig. 4(a) also shows a linear variation of T_e with T_L above 100 K followed by a weaker variation at lower lattice temperatures.

The data of Fig. 4(a) are again plotted in Fig. 4(b) (full and open circles), this time as a function of T_e . Above 70 K, a clear $1/T_e$ dependence is observed, similar to that reported elsewhere.¹ This suggests that what determines the minority carrier mobility is mostly its own temperature, rather than that of majority carriers. This hypothesis can be tested by measuring the T_e -dependence of the mobilities when, as described in Fig. 2(b), T_e is varied by changing the electric field while T_L is held constant. The triangles in Fig. 4(b) correspond to $T_L \approx 35$ K, while the squares correspond to $T_L = 15$ K. For $100 \text{ K} < T_e < 200 \text{ K}$, the mobility dependence is well fitted by a $T_e^{-1.3}$ law. It is striking to see that the

measured mobility values at fixed T_L are close to those obtained when T_L also varies between 50 K and 200 K (circles). This similarity shows that, in this range, the minority carrier mobility weakly depends on T_L . The squares in Fig. 4(b) correspond to $T_L \approx 15$ K and to $T_e < 50$ K. In this range, there is a dramatic increase of mobility, with both electron and spin mobilities being described by a $T_e^{-4.3}$ power law.

The weak dependence of electron mobility on T_L suggests that the mechanism which limits the mobility is scattering by charged impurities and holes, rather than phonon scattering. This conclusion is also supported by theoretical considerations at the high doping levels used here.^{7,8} Considering only scattering by electrical charges, the momentum relaxation time $\langle \tau_m \rangle = \mu_e m^* / q$, where m^* is the effective mass, is written as an average over electron kinetic energy ε of the energy-resolved time $\tau_m(\varepsilon)$. One can write that $\tau_m(\varepsilon) = a(T_L, T_e) \varepsilon^p$, where the exponent p depends on the efficiency of the screening by holes²¹ and where, as found above, the dependence of $a(T_L, T_e)$ on T_L should be weaker than that on T_e . One then finds

$$\langle \tau_m \rangle \propto a(T_L, T_e) \cdot T_e^{-p}. \quad (3)$$

The quantity p is estimated using photoconductivity and photoHall measurements. Using a defocused laser excitation to ensure that the photoelectron concentration is homogeneous over the Hall bar, the ratio $r_H = \mu_e^H / \mu_e$ of the Hall mobility μ_e^H to the drift mobility of minority electrons can be found. The quantity p can then be determined using¹⁸

$$r_H = \frac{\Gamma(5/2 + 2p) \Gamma(5/2)}{[\Gamma(5/2 + p)]^2}. \quad (4)$$

The result is $r_H = 0.95 \pm 0.25$ at $T_e = 95$ K and $r_H = 0.8 \pm 0.25$ at $T_e = 300$ K, in agreement with the values close to unity obtained for majority electrons in n-GaAs.²⁰ Using these values and the graphical representation of Eq. (4) in the inset of Fig. 4(b), p is found to lie between approximately -0.5 and 0.5 , in qualitative agreement with the predictions of the Brooks-Herring model²¹ for screened collisions by charged impurities. The small value of p implies that the measured temperature dependence is mainly that of the prefactor $a(T_L, T_e)$ in Eq. (3).

The origin of the T_e dependence of the minority electron mobility is at present not understood. As suggested by the Brooks-Herring model which considers electron screening,²¹ it is probable that $a(T_L, T_e)$ depends on the screening length, which itself depends on the temperature. At the doping levels considered here, the mobility is likely to be determined by scattering by potential fluctuations caused by the random distribution of ionized acceptors rather than by individual charges. For $T_L = 10$ K, the maximum amplitude of the unscreened potential fluctuations is of the order of 40 meV.²² While some attempts have been made to include the effects of screening on transport,^{7,21,23} a complete description including the effect of both disorder and screening is still out of reach.

This work shows that in developing models for minority carrier mobility, accounting for the hole distribution alone,

as proposed by Ref. 7, it is not possible to describe the observed temperature dependence of the minority electron mobility since significant variations are measured even when the hole temperature is constant. The inclusion of minority carrier statistics in theoretical models is therefore necessary to better understand minority carrier mobilities in doped semiconductors.

- ¹K. Beyzavi, K. Lee, D. M. Kim, M. I. Nathan, K. Wrenner, and S. L. Wright, *Appl. Phys. Lett.* **58**, 1268 (1991).
- ²D. Luber, F. Bradley, N. Haegel, M. Talmadge, M. Coleman, and T. Boone, *Appl. Phys. Lett.* **88**, 163509 (2006).
- ³F. Schultes, T. Christian, R. Jones-Albertus, E. Pickett, K. Alberi, B. Fluegel, T. Liu, P. Misra, A. Sukiasyan, H. Yuen *et al.*, *Appl. Phys. Lett.* **103**, 242106 (2013).
- ⁴S. Kim, C. Son, S. Chung, Y. Park, E. Kim, and S. Min, *Thin Solid Films* **310**, 63 (1997).
- ⁵M. L. Lovejoy, M. R. Melloch, and M. S. Lundstrom, *Appl. Phys. Lett.* **67**, 1101 (1995).
- ⁶W. Walukiewicz, J. Lagowski, L. Jastrzebski, and H. Gatos, *J. Appl. Phys.* **50**, 5040 (1979).
- ⁷T. Kaneto, K. Kim, and M. Littlejohn, *Phys. Rev. B* **47**, 16257 (1993).
- ⁸E. Tea and F. Aniel, *J. Appl. Phys.* **109**, 033716 (2011).
- ⁹C. M. Colomb, S. A. Stockman, S. Varadarajan, and G. E. Stillman, *Appl. Phys. Lett.* **60**, 65 (1992).
- ¹⁰E. S. Harmon, M. L. Lovejoy, and M. R. Melloch, *Appl. Phys. Lett.* **63**, 536 (1993).
- ¹¹I. Favorskiy, D. Vu, E. Peytavit, S. Arscott, D. Paget, and A. C. H. Rowe, *Rev. Sci. Instrum.* **81**, 103902 (2010).
- ¹²T. Furuta, H. Taniyama, and M. Tomizawa, *J. Appl. Phys.* **67**, 293 (1990).
- ¹³N. Okamoto, H. Kurebayashi, T. Trypiniotis, I. Farrer, D. A. Ritchie, E. Saitoh, J. Sinova, J. Masek, T. Jungwirth, and C. H. W. Barnes, *Nat. Mater.* **13**, 932 (2014).
- ¹⁴F. Cadiz, P. Barate, D. Paget, D. Grebenkov, J. P. Korb, A. C. H. Rowe, T. Amand, S. Arscott, and E. Peytavit, *J. Appl. Phys.* **116**, 023711 (2014).
- ¹⁵H. S. Bennett, *J. Appl. Phys.* **92**, 4475 (2002).
- ¹⁶R. K. Ahrenkiel, D. J. Dunlavy, D. Greenberg, H. C. Schlupmann, H. C. Hamaker, and H. F. MacMillan, *Appl. Phys. Lett.* **51**, 776 (1987).
- ¹⁷Y. Qi, Z. G. Yu, and M. E. Flatté, *Phys. Rev. Lett.* **96**, 026602 (2006).
- ¹⁸R. S. Popovic, *Hall Effect Devices* (Institute of Physics Publishing, Bristol, 2004).
- ¹⁹J. Shah, *Ultrafast Spectroscopy of Semiconductors and Semiconductor Nanostructures* (Springer, Berlin, 1999).
- ²⁰D. Look, C. E. Stutz, J. R. Sizelove, and K. R. Evans, *J. Appl. Phys.* **80**, 1913 (1996).
- ²¹D. Chattopadhyay and H. J. Queisser, *Rev. Mod. Phys.* **53**, 745 (1981).
- ²²A. L. Efros, Y. S. Halpern, and B. I. Shklovsky, in *Proceedings of the International Conference on Physics of Semiconductors* (Polish Scientific publishers, Warsaw, 1972).
- ²³D. N. Quang, N. N. Dat, and D. V. An, *Phys. Lett. A* **182**, 125 (1993).